Talanta 182 (2018) 253–258

Contents lists available at ScienceDirect

Talanta

journal homepage: www.elsevier.com/locate/talanta

Nanoparticle-Enhanced Laser Induced Breakdown Spectroscopy for the noninvasive analysis of transparent samples and gemstones

C. Koral[a,1], M. Dell'Aglio[b], R. Gaudiuso[a,b,2], R. Alrifai[a], M. Torelli[c], A. De Giacomo[a,b,*]

[a] Department of Chemistry, University of Bari, Via Orabona 4, 70126 Bari, Italy
[b] Institute of Nanotechnology, CNR-NANOTEC, c/o Department of Chemistry, University of Bari, Via Orabona 4, 70126 Bari, Italy
[c] Centro di Analisi Gemmologiche Masterstones, Via Alessandri 4, 00151 Roma, Italy

ARTICLE INFO

Keywords:
Nanoparticle-Enhanced LIBS
Gemstones
Transparent samples
Non-destructive analysis

ABSTRACT

In this paper, Nanoparticle-Enhanced Laser Induced Breakdown Spectroscopy is applied to transparent samples and gemstones with the aim to overcome the laser induced damage on the sample. We propose to deposit a layer of AuNPs on the sample surface by drying a colloidal solution before ablating the sample with a 532 nm pulsed laser beam. This procedure ensures that the most significant fraction of the beam, being in resonance with the AuNP surface plasmon, is mainly absorbed by the NP layer, which in turn results the breakdown to be induced on NPs rather than on the sample itself. The fast explosion of the NPs and the plasma induction allow the ablation and the transfer in the plasma phase of the portion of sample surface where the NPs were placed. The employed AuNPs are prepared in milliQ water without the use of any chemical stabilizers by Pulsed Laser Ablation in Liquids (PLAL), in order to obtain a strict control of composition and impurities, and to limit possible spectral interferences (except from Au emission lines). Therefore with this technique it is possible to obtain, together with the emission signal of Au (coming from atomized NPs), the emission spectrum of the sample, by limiting or avoiding the direct interaction of the laser pulse with the sample itself. This approach is extremely useful for the elemental analysis by laser ablation of high refractive index samples, where the laser pulse on an untreated surface can otherwise penetrate inside the sample, generate breakdown events below the superficial layer, and consequently cause cracks and other damage. The results obtained with NELIBS on high refractive index samples like glasses, tourmaline, aquamarine and ruby are very promising, and demonstrate the potentiality of this approach for precious gemstones analysis.

1. Introduction

Laser Induced Breakdown Spectroscopy has proved a valuable tool for glass [1,2] and gemstone analysis [3–6], in particular for gem provenance studies [7] and to discriminate between different minerals [8]. The main advantages of using LIBS for glass and for gemstones analysis is that it is possible to have multispectral information just by a single shot, which enables fast multi-elemental analysis [9]. Moreover, the feasibility of calibration free approaches has also been demonstrated for these samples, which is especially useful when it is hard or expensive to produce matrix matched standards, like in the case of gemstones [10]. One of the crucial questions in applying laser ablation-based methods to the analysis of transparent samples is related to their high refractive index. This causes the laser pulse to penetrate beyond the superficial layer, thus inducing cracks and damage in the sample itself [11,12]. This drawback prevents a straightforward application of LIBS to precious transparent samples such as gemstones or ancient glass although the use of UV laser pulse can limit the surface damage due to the better coupling of the laser with the matrix. Recently, the use of metallic NPs for controlling the laser-matter interaction has been proposed by the same authors of the present paper. It has been demonstrated for metallic samples [13] and microdrops of solutions [14] that the laser pulse, off-resonance with the NPs surface plasmons, can induce the collective oscillation of NP surface electrons, which in turn results in local field enhancement and in LIBS signal improvement. The use of NPs for enhancing the LIBS signal and analytical performance is named Nanoparticle-Enhanced LIBS, (NELIBS) [15]. In this paper, a NP layer was deposited on the transparent sample surface, in order to avoid the direct interaction of the laser pulse with the transparent medium. To prevent the direct laser interaction with the sample, a laser pulse in

* Corresponding author at: Department of Chemistry, University of Bari, Via Orabona 4, 70126 Bari, Italy.
E-mail address: alessandro.degiacomo@uniba.it (A. De Giacomo).
[1] Present address: Department of Physics, University of Napoli, Federico II Monte Sant'Angelo 80126, Napoli.
[2] Present address: University of Massachusetts Lowell, 265 Riverside Street, Lowell MA 01854, USA.

https://doi.org/10.1016/j.talanta.2018.02.001
Received 7 December 2017; Received in revised form 29 January 2018; Accepted 1 February 2018
Available online 20 February 2018
0039-9140/

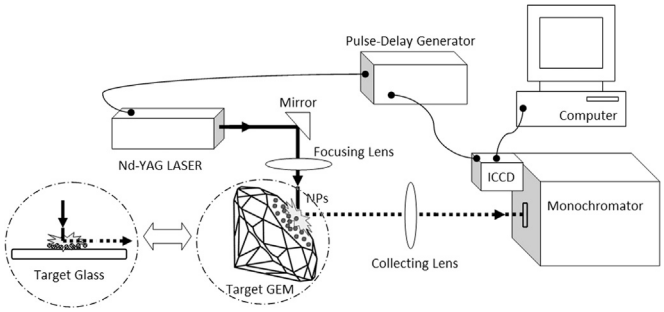

Fig. 1. Experimental set-up.

resonance with the surface plasmon of the NPs was employed, so that most of the laser energy was absorbed by the NPs. The preferential absorption of laser photons by the NPs allowed induction of the breakdown on the NPs layer deposited on the sample surface, rather than directly on the sample surface. As a consequence of this phenomenon and of the NP explosion, only a few superficial layers of sample were transported in the plasma phase. The main result was therefore not only to prevent the sample cracking, but also to avoid visible damage on the sample surface after the NELIBS measurement. Finally, in order to acquire an emission spectrum that was representative of the elemental composition of the sample without any interference, except for the emission lines of the metal of NPs, the NPs were synthetized in milliq water by Pulsed Laser Ablation in Liquids (PLAL) [16] without any kind of stabilizer or chemical contaminant.

2. Materials and methods

The experimental set up (Fig. 1) includes a second harmonic Nd:YAG laser, Quantel Q-smart 850 (532 nm, 6 ns duration, energy up to 500 mJ), a spectroscopic system consisting of a Czerny-Turner spectrograph (JY Triax 550) coupled with an ICCD (JY 3000) which was synchronized with the Pockels cell of the laser source by a pulse generator (Stanford DG 535). The sample was mounted on a microstage holder with adjustable angle with respect to the laser direction. The laser was focused 5 mm beyond the sample with a planoconvex lens with a 100 mm focal length, in order to avoid the breakdown on the sample surface. At this experimental condition the laser spot was around 1.5 mm of diameter. The laser was used in single shot mode and the parameters were as follows: delay time after the laser pulse was 800 ns and gate width was 10 μs (virtually an integrated time LIBS measurement).

The AuNPs were prepared by Pulsed Laser Ablation in Liquid (PLAL) as described in Ref. [17]. PLAL allows ultrapure NPs to be produced in milliq water without the use of any chemical stabilizers. This is an important point in NELIBS applications because the emission signal of all the impurities of the colloidal solution are strongly enhanced and the spectrum of contaminants may affect the elemental analysis of the sample. The produced AuNPs, characterized with SPR (Surface Plasmon Resonance), TEM (Transmission Electron Microscopy), and DLS (Dynamics Light Scattering), had diameter of 15 ± 2 nm. The SPR of AuNPs deposited on quartz substrate after drying the drops of colloidal solution for the NELIBS experiment is reported in Ref. [14]. The concentration of the Au colloidal solution used in this work was between 0.05 and 0.6 g/l, depending on the experiment, as reported in the figure captions. The film of NPs on the sample surface were obtained by depositing and drying several drops of the colloidal solution until they formed a visible layer on the surface. The sample was placed on the holder and the angle between the laser direction and the sample surface was adjusted in order to have the maximum reflection at low laser energy below the breakdown threshold. Once the optimal angle was found, the energy of the laser was set up between 100 and 200 mJ in order to induce the breakdown of the deposited NP film.

Optical microscope images of glass and gemstones were acquired with Dino-Lite pro (AM431ZTA).

The following samples were tested: microscope glass slides (7101 Pearl); Pyrex glass; standards of di-lithium tetraborate doped with Cr_2O_3 with Cr concentration varying from 0.0017 to 0.1 wt% provided by CRITT Matériaux Alsace – Schiltigheim – France; tourmaline from the Royal Mineralogical Museum of Naples; aquamarine and ruby provided by *Centro di Analisi Gemmologiche "Masterstones"* of Rome.

2.1. Glass samples

Glass slides of different typologies were tested with NELIBS with the laser beam perpendicular to the sample surface. A gold colloidal solution was deposited on the glass, in order to obtain a thin layer of NPs. The laser was focused beyond the sample surface in order to have a laser spot of 1.5 mm and a fluence of 1.5 J cm^{-2}, as shown in Fig. S1 of Supplementary material. This energy was below the breakdown threshold of the sample and without the deposition of NPs the laser would pass through the sample without inducing any breakdown. On the contrary, when the sample was covered with the AuNPs, the efficient laser absorption by the NP surface electrons produced the breakdown of the NP layer, and the emission spectrum of the NPs and of the underlying portion of sample was obtained, as reported in Fig. 2. Unlike in previous NELIBS applications [13,14], in this case, in order to maximize the photon absorption of the Au-NPs, whose surface plasmon resonance is around 523 nm (Fig. S2 of Supplementary material), we used the second harmonic of the Nd:YAG, 532 nm, to obtain an effective match with the NP band absorption. The efficient laser absorption from the NPs allows the laser pulse to induce the breakdown directly on the NPs, avoiding the direct interaction of the laser pulse with the sample.

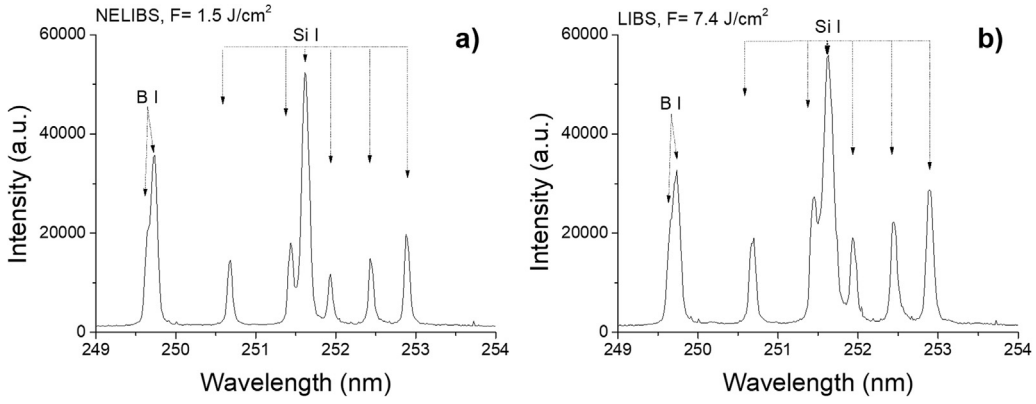

Fig. 2. a) NELIBS and b) LIBS spectra of borosilicate glass. Different laser fluences were employed in order to obtain comparable emission spectra: 1.5 J cm^{-2} and 7.4 J cm^{-2} respectively, in the case of NELIBS 3 drops of 2 μl of AuNPs solution 0.05 g/l.

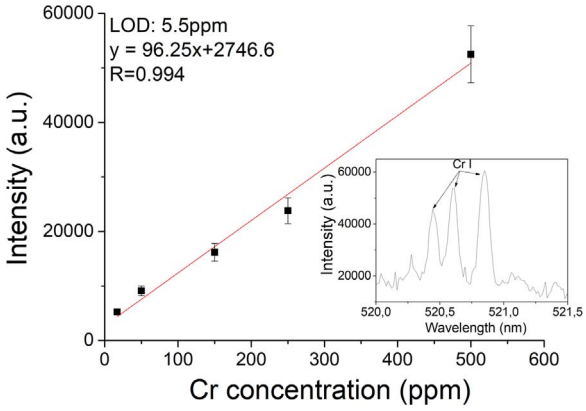

Fig. 3. NELIBS calibration curve of Cr built by using Cr glass standards provided by CRITT. (The experimental conditions are: Fluence 1.8 J cm^{-2}, spot size 1.5 mm, 3 drops of 2 µl of AuNP solution, 0.05 g/l). In the inset a frame of NELIBS spectrum of Cr I is shown.

In this way, the preferential breakdown of NPs occurred, and only the portion of the sample surface that was in contact with the NPs was ablated and transported in the plasma phase. In these NELIBS experiments, a lower amount of sample material is ablated than in conventional LIBS. Nevertheless, the effect of field enhancement induced locally on the NPs, allows the acquisition of an emission signal completely comparable with the one obtained with conventional LIBS, with the advantage of inducing a negligible damage on the sample surface.

Fig. 2 shows the spectra obtained by NELIBS and LIBS on Pyrex glass (borosilicate glass), respectively. As Fig. 2 shows, in order to obtain NELIBS and LIBS spectra with comparable intensity, it was necessary to use 5 times higher laser fluence for LIBS experiment. The net result was that, by using different laser fluences for the two experiments, the damage induced on the glass surface was clearly visible with LIBS, while no visible damage was present in the case of NELIBS, as shown in Fig. S3 of Supplementary material.

The inset of Fig. 3 shows the NELIBS spectrum frame relative to chromium as obtained from the analysis of green glass (taken from commercially available beverage bottle). In order to estimate the LOD of NELIBS at these experimental conditions, a calibration curve for Cr was drawn with a set of glass standards, and is shown on Fig. 3. The LOD for Cr, estimated as the ratio between the slope of the calibration curve and the background standard deviation multiplied by a factor of 3, was found to be 5.5 ppm in these experiments. It is important to underline that this LOD is not better than what is generally obtained with conventional LIBS but in this case, the spectral information was achieved without inducing any visible damage on the sample surface. In a previous work of ours [13] we have reported a SEM investigation demonstrating that the damage induced on silicon and glass during NELIBS consists of several craters with average size of the same order of the NP diameters, and is thus not visible by conventional optical microscopy.

In this configuration, i.e. when the laser is focused perpendicular to the sample surface, in cases when the sample is not a slide, it can happen that the portion of laser pulse that is not stopped by the breakdown of the NPs, passes inside the sample. Since the sample has a higher refractive index than air, this transmitted portion can induce a damage inside the sample. This drawback can be crucial when the elemental analysis is performed on precious transparent samples, like gemstones, that should be preserved as much as possible.

2.2. Gemstone samples

In previous works of ours [5,10] we have demonstrated the feasibility of LIBS for gemstone elemental analysis and to obtain important mineralogical information. In those experiments, LIBS was applied on raw gemstones, so that, in most cases, LIBS was able to produce an efficient spark directly on the gemstone surface.

The first case of gemstones analysis presented here is a tourmaline sample, $Na(Al,Fe,Li)Al_6(Si_6O_{18})(BO)_3(F, OH)_4$, that we analyzed both with LIBS and NELIBS. The LIBS measurements performed in scanning mode (10 laser pulses averaged in each acquired spectral window), have been already published in a previous work of ours [5]. Fig. 4(a) shows the sample after the LIBS analysis, and the two stripes of craters due to the laser ablation are clearly evident. Fig. 4(b) shows the sample after the deposition of AuNPs and after the single shot NELIBS measurement. Fig. 4(b) shows very clearly that after NELIBS there is no visible damage. Fig. 5 compares two frames of emission spectrum as obtained with NELIBS and LIBS at the same experimental conditions (single shot, same laser fluence) and it can be noted that the NELIBS signal is, as usual, enhanced by more than one order of magnitude. The NELIBS enhancement is related to the fact that the laser pulse induces a coherent oscillation of the conduction electrons in small metallic particles, which in turn amplifies the incident electromagnetic field by locally increasing the electric field near the particle surface. This effect results in a more efficient ignition and excitation of the plasma and in a more confined plasma, as discussed in Ref. [15]. To check if the ablation is stoichiometric also in NELIBS, like in conventional LIBS, we tested a Calibration Free approach (CF) [5,18] with the NELIBS spectrum in order to determine the *apfu* (atoms per formula unit) of the main elements present in the tourmaline, Al, Si and B. First of all, as already described in [5], plasma temperature and electron density were determined by the Boltzmann plot of Fe I emission lines and Stark broadening of Fe I (426.05 nm) emission line, respectively. The Boltzmann plot was linearly fitted with an $R^2 = 0.989$, and the measured values of temperature and electron density were 5200 ± 500 K and $3.9*10^{16} \pm 9*10^{15}$ cm^{-3}, respectively. The existence of a Boltzmann distribution and high value of electron density (which fulfils the McWhirter criterion) can validate the assumption of local thermodynamic equilibrium also for the NELIBS plasma produced at the present experimental conditions. The CF approach was then applied for the

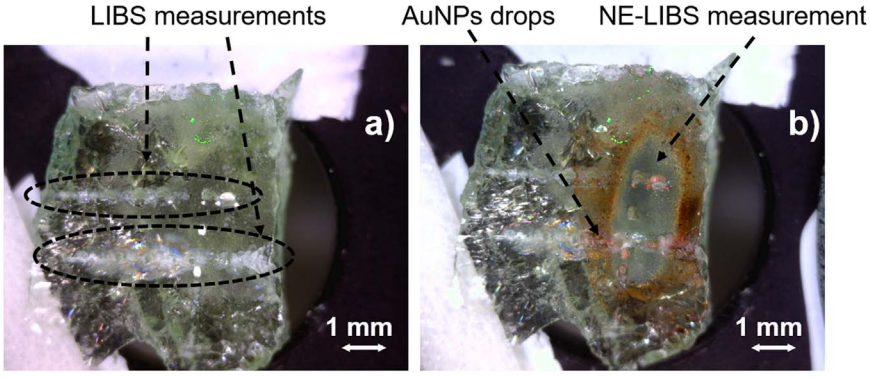

Fig. 4. Tourmaline sample a) after a conventional LIBS measurement; b) after NP deposition (2 drops of 2 µl of AuNP solution 0.6 g/l) followed by single shot NELIBS measurement. Experimental conditions: laser-surface incidence angle 28°, laser fluence 7.6 J cm^{-2}. In a) the two stripes of craters due to the laser ablation of LIBS measurements have been highlighted with dashed lines.

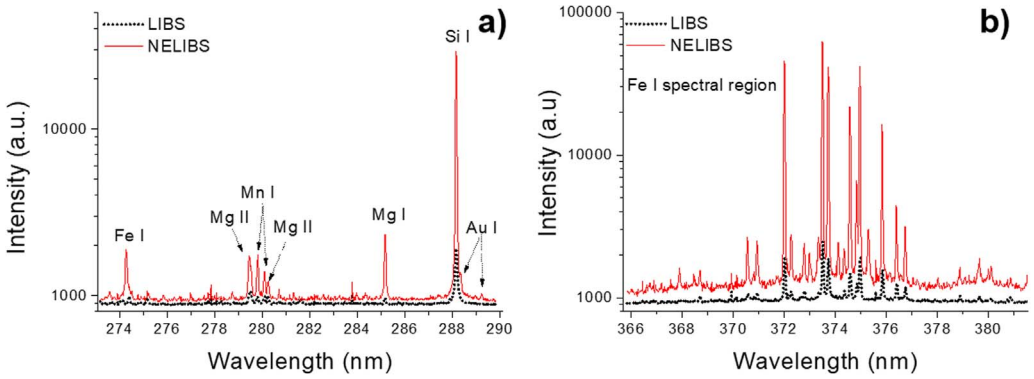

Fig. 5. a) and b) Emission spectra of tourmaline sample with LIBS (black) and NELIBS (red). The experimental conditions are: Fluence 7.6 J cm^{-2} in the case of NELIBS 2 drops of 2 μl of AuNPs solution 0.6 g/l.

Table 1
Certified and Calibration Free NELIBS *apfu*. For the calibration free the temperature and electron number density were calculated from atomic iron lines and are: T = 5200 K, Ne = 3.9e16 cm^{-3}.

Elements	*apfu* (conventional techniques [5])	*apfu* (NELIBS on the basis of 6 Si)
Si	6.187	6
Al	7.372	7.252
B	2.662	3.150

element quantification. In particular, after the calculation of the total atomic number densities of Al, Si and B, the *apfu* of Si was fixed to 6 (based on the know formula of tourmaline), while the other two *apfu* were calculated on the basis of the elemental ratios Al/Si and B/Si. The results are reported in Table 1, which shows a good agreement between NELIBS and certified analytical techniques [5] and confirms the feasibility of the proposed technique.

When the stone is carved and its surface is polished, applying LIBS can be very dangerous for the sample integrity, and the cost of the stone may discourage the application of LIBS for this task. Indeed if a portion of laser beam not stopped by the breakdown of the NPs penetrates inside the sample, since the refractive index of the stone is higher than that one of the air and the surface is flat, the beam can be reflected inside the stone several times, and finally be focused inside the stone. This can induce an internal damage, as shown in the example reported in Fig. S4 of Supplementary material, and in turn decrease the value of the stone. For this reason after the deposition of the NPs on the sample surface of a gemstones, in this work the surface of the sample was tilted with respect to the incident laser beam direction. In Fig. 6 the optical transmission of NPs film deposited on a high-refractive index glass is reported as a function of the angle between the laser direction and the sample surface. Fig. 6 shows clearly that it is possible to find an optimal angle for performing NELIBS and for minimizing the transmitted portion of laser pulse to the sample, which in these experiments was found to be for angles smaller than 30°. Ideally the maximum reflectance (i.e. the minimum transmittance) is obtained for angles close to 0°, but as a portion of the pulse is needed for inducing the breakdown, a higher incidence angle is required for the NELIBS experiment. In this frame, the small-angle laser irradiation allows most of the laser pulse to be reflected and therefore not used for the breakdown of the NP film. For this reason, preliminary experiments with laser energy below the breakdown threshold were performed to find the best incidence angle.

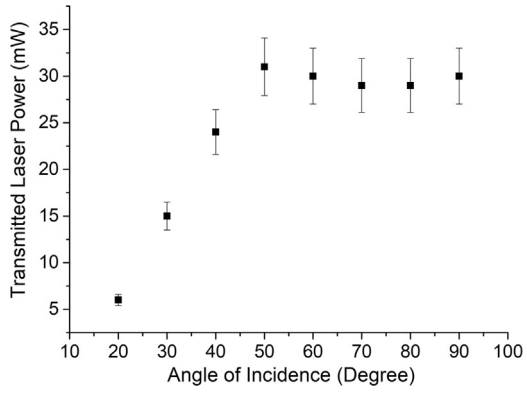

Fig. 6. Laser transmitted power beyond the NPs film as a function of the angle between the sample surface and the laser direction.

Fig. 7(a)-(d) shows that after NELIBS measurements of an aquamarine sample (the blue variety of beryl, with formula $Be_3Al_2Si_6O_{18}$), no visible damage is induced on the facet of the gemstone, and, after NP removal, the stone looks exactly as it did before the treatment.

The corresponding emission spectra of the single shot experiments are reported in Fig. 7(e) and (f) and show that, together with the emission lines of Au I, coming from the NPs, the transitions of elements from the sample are clearly detected. Indeed the spectra are characterized by features from the major elements, like Be, Al and Si, and from trace elements, like Fe and Ca. The presence of Fe as a trace element gives the blue color tonality to the aquamarine [19].

The same experiment was performed on a ruby (corundum red type), Al_2O_3, as shown in Fig. 8(a)-(d).

Also in this case the damage on the facet of the ruby is not visible, although the trace element determining the color of the gemstone, Fe and Cr, are clearly detected, as shown in Fig. 8(e) and (f). The red color of corundum is due to traces of trivalent Cr cause that can replace Al in the crystal structure [20].

3. Conclusion

NELIBS on transparent media, like glass and gemstones, was presented in this work. It was pointed out that the deposition of a thin layer of NPs on the sample surface can avoid visible damage on the sample, when the laser pulse is in resonance with the NP surface plasmon. When a resonant laser pulse irradiates the NPs, most of its energy is absorbed by the NPs, thus inducing the preferential ablation of the particles rather than the breakdown of the underlying the substrate, which in turns prevents a direct interaction of the laser pulse with the sample.

In the case of carved gemstones, in order to avoid any potential damage induced from the transmitted residual laser pulse, the tilting of the sample surface was proposed. The angle between the surface and the laser incidence direction was adjusted in order to find a compromise between the necessary irradiance for inducing the breakdown of the NPs layer and the necessity of minimizing the transmitted portion of the residual laser beam after the induced breakdown of the NPs layer.

The results show that with this technique it is possible to perform

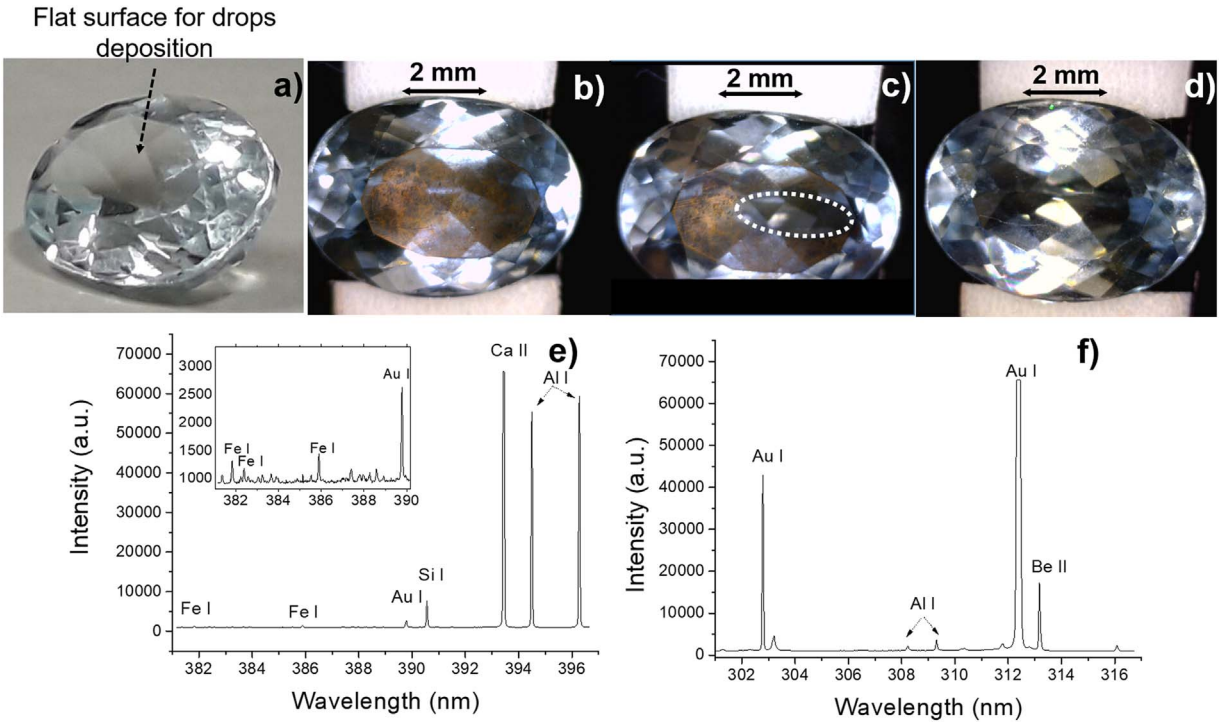

Fig. 7. Diamond cut aquamarine sample: a) before the treatment, b) after NP deposition, c) after the laser shot, d) after NP removal. a) photo of aquamarine; b), c) and d) optical microscope images acquired perpendicularly to the flat surface; e) and f) two single shot NELIBS spectra of aquamarine. Experimental conditions: laser-surface incidence angle 28°, laser fluence 7.6 J cm^{-2}, NP concentration: 6 drops of 2 µl of AuNPs solution 0.6 g/l.

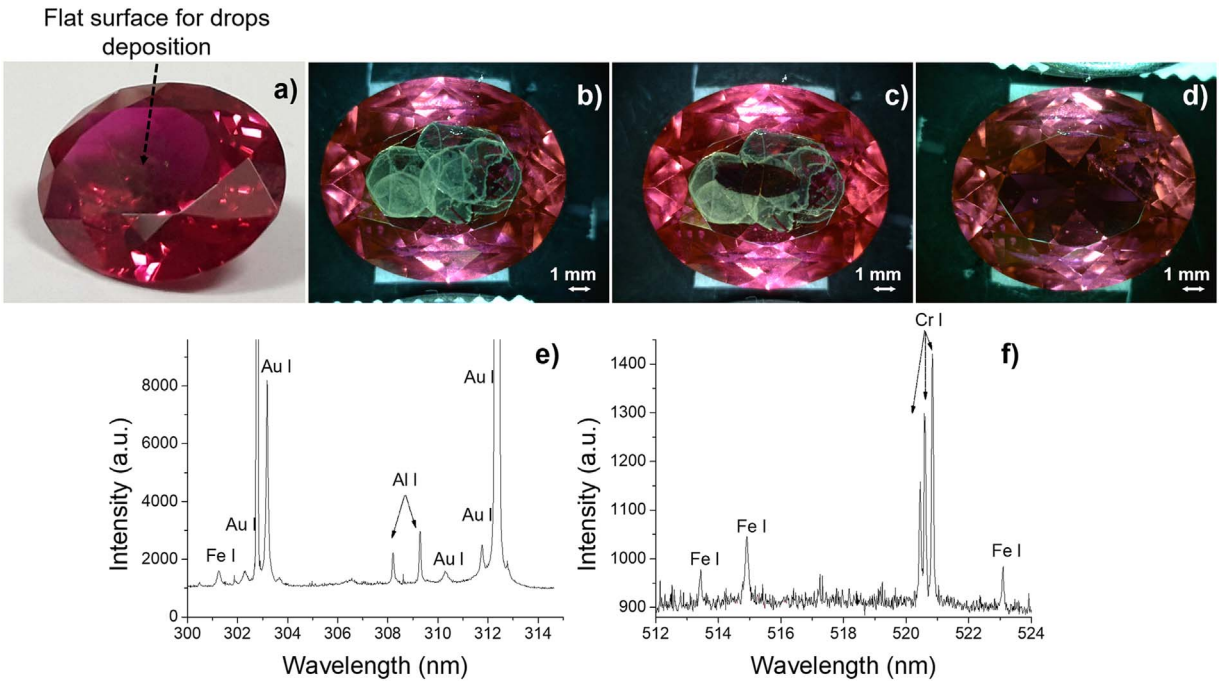

Fig. 8. Diamond cut ruby sample: a) before the treatment, b) after the NPs deposition, c) after the laser shot, d) after NPs removal. a) photo of aquamarine; b), c) and d) optical microscope images, acquired perpendicularly to the flat surface.; e) and f) two single shot NELIBS spectra of ruby, Experimental conditions: laser-surface incidence angle 28°, laser fluence 7.6 J cm^{-2}, NPs concentration 3 drops of 10 µl of AuNPs solution 0.6 g/l.

the elemental analysis of the gemstone with the same, or even better, performance of conventional LIBS, with the additional important result of preventing the sample damage.

Acknowledgments

All the research activity has been developed in the Department of Chemistry of the University of Bari in the ALPA (Advanced Laser Plasma Applications) Lab under the project MIUR-Apulia Space co-ordinated by Prof A. De Giacomo.

The authors would like to thank Dr. Frédéric Pelascini (CRITT Matériaux Alsace – Schiltigheim – France) for the green glass standards and Dr. Manuela Rossi and Prof. Maria Rosaria Ghiara (Royal Mineralogical Museum, Museum Centre of Natural and Physical

Sciences, University of Naples “Federico II”, Naples) for the tourmaline sample.

Appendix A. Supporting information

Supplementary data associated with this article can be found in the online version at http://dx.doi.org/10.1016/j.talanta.2018.02.001.

References

[1] C. Gerhard, J. Hermann, L. Mercadier, L. Loewenthal, E. Axente, C.R. Luculescu, T. Sarnet, M. Sentis, W. Viol, Quantitative analyses of glass via laser-induced breakdown spectroscopy in argon, Spectrochim. Acta B 101 (2014) 32–45.

[2] U. Panne, C. Haisch, M. Clara, R. Niessner, Analysis of glass and glass melts during the vitrification process of fly and bottom ashes by laser-induced plasma spectroscopy. Part I: normalization and plasma diagnostics, Spectrochim. Acta B 53 (1998) 1957–1968.

[3] R.S. Harmon, F.C. De Lucia, C.E. McManus, N.J. McMillan, T.F. Jenkins, M.E. Walsh, A. Miziolek, Laser-induced breakdown spectroscopy, An emerging chemical sensor technology for real-time field-portable, geochemical, mineralogical, and environmental applications, Appl. Geochem. 21 (2006) 730–747.

[4] G. Agrosì, G. Tempesta, E. Scandale, S. Legnaioli, G. Lorenzetti, S. Pagnotta, V. Palleschi, A. Mangone, M. Lezzerini, Application of Laser Induced Breakdown Spectroscopy to the identification of emeralds from different synthetic processes, Spectrochim. Acta B 102 (2014) 48–51.

[5] M. Rossi, M. Dell’Aglio, A. De Giacomo, R. Gaudiuso, G.S. Senesi, O. De Pascale, F. Capitelli, F. Nestola, M.R. Ghiara, Multi-methodological investigation of kunzite, hiddenite, alexandrite, elbaite and topaz, based on laser induced breakdown spectroscopy and conventional analytical techniques for supporting mineralogical characterization physics and chemistry of minerals, Phys. Chem. Miner. 41 (2014) 127–140.

[6] R.S. Harmon, R.E. Russo, R.R. Hark, Applications of laser-induced breakdown spectroscopy for geochemical and environmental analysis: a comprehensive review, Spectrochim. Acta B 87 (2013) 11–26.

[7] C.E. McManus, N.J. McMillan, R.S. Harmon, R.C. Whitmore, F.C. DeLucia, A.W. Miziolek, The use of laser induced breakdown spectroscopy (LIBS) in the determination of gem provenance beryls, Appl. Opt. 47 (2008) 72–79.

[8] D.C. Alvey, K. Morton, R.S. Harmon, J.L. Gottfried, J.J. Remus, L.M. Collins, M.A. Wise, LIBS-based geochemical fingerprinting for the rapid analysis and discrimination of minerals the example of garnet, Appl. Opt. 49 (2010) C168–C180.

[9] D.W. Hahn, N. Omenetto, Laser-induced breakdown spectroscopy (LIBS), Part II: review of instrumental and methodological approaches to material analysis and applications to different fields, Appl. Spectrosc. 66 (2012) 347–419.

[10] A. De Giacomo, M. Dell'Aglio, R. Gaudiuso, A. Santagata, G.S. Senesi, M. Rossi, M.R. Ghiara, F. Capitelli, O. De Pascale, A Laser Induced Breakdown Spectroscopy application based on Local Thermodynamic Equilibrium assumption for the elemental analysis of alexandrite gemstone and copper-based alloys, Chem. Phys. 398 (2012) 233–238.

[11] Y. Kanemitsu, Y. Tanaka, Mechanism of crack formation in glass after high-power laser pulse irradiation, J. Appl. Phys. 62 (1987) 1208.

[12] C. Barnett, E. Cahoon, J.R. Almirall, Wavelength dependence on the elemental analysis of glass by Laser Induced Breakdown Spectroscopy, Spectrochim. Acta B 63 (2008) 1016–1023.

[13] A. De Giacomo, R. Gaudiuso, C. Koral, M. Dell'Aglio, O. De Pascale, Nanoparticle enhanced laser induced breakdown spectroscopy: effect of nanoparticles deposited on sample surface on laser ablation and plasma emission, Spectrochim. Acta B 98 (2014) 19–27.

[14] A. De Giacomo, C. Koral, G. Valenza, R. Gaudiuso, M. Dell’Aglio, Nanoparticle enhanced laser-induced breakdown spectroscopy for microdrop analysis at subppm level, Anal. Chem. 88 (2016) 5251–5257.

[15] A. De Giacomo, M. Dell'Aglio, R. Gaudiuso, C. Koral, G. Valenza, Perspective on the use of nanoparticles to improve LIBS analytical performance: Nanoparticle enhanced laser induced breakdown spectroscopy (NELIBS), J. Anal. At. Spectrom. 31 (2016) 1566–1573.

[16] S. Barcikowski, G. Compagnini, Advanced nanoparticle generation and excitation by lasers in liquids, Phys. Chem. Chem. Phys. 15 (2013) 3022–3026.

[17] M. Dell'Aglio, V. Mangini, G. Valenza, O. De Pascale, A. De Stradis, G. Natile, F. Arnesano, A. De Giacomo, Silver and gold nanoparticles produced by pulsed laser ablation in liquid to investigate their interaction with ubiquitin, Appl. Surf. Sci. 374 (2016) 297–304.

[18] V.S. Burakov, S.N. Raikov, Quantitative analysis of alloys and glasses by a calibration-free method using laser-induced breakdown spectroscopy, Spectrochim. Acta B 62 (2007) 217–223.

[19] N.J. McMillan, C.E. McManus, R.S. Harmon, F.C. DeLucia, A.W. Miziolek, Laser-induced breakdown spectroscopy analysis of complex silicate minerals-beryl, Anal. Bioanal. Chem. 385 (2006) 263–271.

[20] S.K. Ho, Analysis of impurity effects on the coloration of corundum by laser-induced breakdown spectroscopy (LIBS), Appl. Spectrosc. 69 (2015) 269–276.